**RESEARCH PAPER**

# Study on the applicability of a modified strain approach to predict the fatigue life of HFMI-treated transverse stiffeners under variable amplitude loading

Daniel Löschner[1] · Imke Engelhardt[1] · Thomas Nitschke-Pagel[2] · Thomas Ummenhofer[3]

## Abstract

This paper analyses the applicability of a modified strain approach to predict the fatigue life of HFMI-treated transverse stiffeners under variable amplitude loading (VAL) with random load sequences of a p(1/3) and linear shaped spectrum. Local stresses are determined using linear-elastic finite element analyses. The measured weld geometry and component imperfections are considered. From the hardness of the HFMI-treated zone and the base material, the elastic–plastic material behaviour and Coffin-Manson parameters to describe the damage parameter Woehler curve are estimated. Based on a hysteresis counting method (HCM), the damage for each closed hysteresis is calculated. The applied notch strain approach includes the impact of residual stresses and the influence of surface roughness. Thus far, the application of similar approaches has only been validated for welded components with comparatively low residual stresses and HFMI-treated welds subjected to constant amplitude loading. To validate the accuracy of the approach for HFMI-treated welds under variable amplitude loading, the approximated fatigue life is compared to the number of cycles derived from experimental investigations. In this study, it is shown in conjunction with experimental results that it is essential to consider the strength of the base material near the weld when assessing the service life. This area can be more critical than the HFMI-treated weld toe.

## Nomenclature

| | |
|---|---|
| a | Weld throat thickness |
| AW | As-welded |

✉ Daniel Löschner
loeschner.daniel@hm.edu

Imke Engelhardt
imke.engelhardt@hm.edu

Thomas Nitschke-Pagel
t.pagel@tu-braunschweig.de

Thomas Ummenhofer
thomas.ummenhofer@kit.edu

[1] Institute for Material and Building Research, University of Applied Science, Munich, Germany

[2] Institute of Joining and Welding, Technische Universität Braunschweig, Braunschweig, Germany

[3] KIT Steel and Lightweight Construction, Research Institute for Steel, Wood and Stone, Karlsruhe, Germany

| | |
|---|---|
| b | fatigue strength exponent |
| BM | Base Material |
| c | fatigue ductility exponent |
| CAL | Constant amplitude loading |
| D | Specified damage sum |
| $D_{real}$ | Real, experimentally determined damage sum |
| E | Young's modulus |
| ε | Strain |
| $\varepsilon_f'$ | fatigue ductility coefficient |
| $H_0$ | Spectrum length |
| HAZ | Heat-affected zone |
| HB | Brinell hardness |
| HFMI | High-Frequency Mechanical Impact Treatment |
| HV | Vickers hardness |
| IIW | International Institute of Welding |
| K' | Cyclic strain hardening coefficient |
| LS | Logitudinal stiffeners |
| $L_S$ | Spectrum length |
| m | Slope above the knee point of the S-N curve |
| m′ | Slope below the knee point |

| $M_\sigma$ | Mean stress sensitivity |
|---|---|
| N | Load cycles |
| $N_{f,exp}$ | Experimentally determined service life to failure |
| $N_{calc}$ | Calculated service life |
| n' | Cyclic strain hardening exponent |
| $n_{bm}$ | Fracture mechanics support factor |
| $P_{RAM}$ | Damage parameter |
| $P_{SWT}$ | Damage parameter |
| $\Theta$ | Weld flank angle |
| R | Stress ratio |
| $r_{HFMI}$ | Weld toe radius in the HFMI-treated state |
| $R_m$ | Tensile strength |
| $R_e$ | Yield strength |
| $R_z$ | Mean surface roughness |
| S-N | Nominal stress range S versus cycles to failure N |
| SCF, $K_t$ | Stress concentration factor |
| $\sigma_{a,i}$, $\sigma_{a,max}$ | Current and maximum stress amplitude |
| $\Delta\sigma_n, \sigma_n$ | Nominal stress range, nominal stress |
| $\Delta\sigma_{eq}$ | Equivalent stress range |
| $\sigma_f'$ | fatigue strength coefficient |
| $\sigma_{RS}^T$ | Transverse residual stress |
| $t'_{HFMI}$ | Indentation depth |
| TS | Transverse attachments |
| UML | Uniform Material Law |
| VAL | Variable amplitude loading |
| $z_1$, $z_2$ | Side length of the fillet weld |

## 1 Introduction

In 2016, the International Institute of Welding (IIW) issued recommendations regarding the application and fatigue assessment of High-Frequency Mechanical Impact (HFMI) treated welds [1] under both constant (CAL) and variable amplitude loading (VAL). This guideline is based on extensive studies that confirmed the potential for improving the fatigue life of welds through the application of HFMI treatment. Whereby the basis of this recommendation is largely derived from fatigue test results of the studies in [2, 3]. It provides a summary of the results of previous studies and assesses the improvement in fatigue strength under CAL as a function of steel grade, welded detail and stress ratio. For the more common case of a VAL, the assessment can be performed via a transformation of the load history into a damage equivalent stress range. The value of the stress range is based on rainflow counting and the modified Palmgren-Miner rule.

$$\Delta\sigma_{eq} = \left( \frac{1}{D} \cdot \frac{\sum \left( \Delta\sigma_i^m \cdot n_i \right) + \Delta\sigma_k^{(m-m')} \cdot \sum \left( \Delta\sigma_j^{m'} \cdot n_j \right)}{\sum n_i + \sum n_j} \right)^{\frac{1}{m}}$$
(1)

The equivalent stress range $\Delta\sigma_{eq}$ is calculated via the specified damage sum D, the stress range $\Delta\sigma_i$ and the slope m above the knee point of the S-N curve, the stress range $\Delta\sigma_j$ and the slope m' below the knee point of the S-N curve, the number of load cycles $n_i$ applied at $\Delta\sigma_i$, the number of load cycles $n_j$ applied at $\Delta\sigma_j$, and the stress range $\Delta\sigma_k$ at the knee point of the S-N curve. In [4], the applicability of Eq.(1) was confirmed for HFMI-treated longitudinal stiffeners (LS) made of S700 subjected to VAL with a linear-shaped spectrum at a stress ratio of R = -1. The spectrum length was set to $H_0 = 250,000$ cycles. It could be shown that a specified damage sum of D = 1 in Eq. (1) can be used to correlate VAL and CAL fatigue data for welds improved using HFMI. However, the allowable value of the specified damage sum is still being discussed. In [5], a specified damage sum of 0.5 is recommended for the fatigue assessment of untreated welds subjected to VAL. A lower value of D = 0.2 is proposed for load spectra with high mean stress fluctuations. In the case of HFMI-treated weld seams, an allowable damage of 0.5 is stated in [1].

The fatigue test data of HFMI-treated transverse attachments (TS) of S355 subjected to blocked VAL at R = 0.1 in [6] resulted in damage sums beneath $D_{real} = 1.0$ and closer to the recommended value of D = 0.5 in [5]. Leitner et al. [7] focused on the fatigue assessment of HFMI-treated steel joints under VAL. Four different test data sets of butt welds and LS tested with randomly distributed VAL were included. It was concluded that assuming a specified damage sum of D = 0.5 to D = 1.0 using the proposed S–N curves for HFMI-treated welds can lead to a conservative fatigue life estimation. The analysis of the results from fatigue tests in [8] on HFMI-treated TS (S355J2+N) reveals that real damage sums in the case of a random load sequence with a p(1/3) spectrum may range between $D_{real}$ = 4 and 120. If the accumulation is based on an experimental S-N curve, the damage sums yield values of $D_{real} < 1$. According to Haibach [7], the inaccuracy of the Miner rule is caused by the fact that sequence effects and thus possible interactions of large, medium and small stresses during VAL are not considered in the damage calculation. Thus, the impacts of the load sequence, overloads and residual stresses on the service life cannot be considered. This might explain the different damage sums determined in the studies mentioned.

With a fatigue assessment based on cyclic elastic–plastic material behaviour, however, a promising approach for considering sequence effects is available. Rudorffer et al. [9] showed that using the notch strain approach and applying the adjusted FKM-guideline "nonlinear" [10], the fatigue life of welded steel components subjected to CAL can be assessed. Additionally, to adjust the damage S-N curve to welds, the estimation of the cyclic material properties via the hardness was adapted. The hardness of the

heat-affected zone (HAZ) is used for fatigue assessment. Lihavainen and Marquis [11] applied a two-stage model to estimate the fatigue life of HFMI-treated LS subjected to CAL. The model includes a local strain approach and linear elastic fracture mechanics. They accounted for compressive residual stresses and geometry improvement based on measured values. Cyclic material properties were estimated via the Uniform Material Law (UML) assuming base material behaviour. Dürr [12] applied a similar approach for HFMI-treated TS of mild (S355) and high-strength steels (S690). He used the model "thin edge layer" [13] to consider residual stresses. In [14], a two-stage model was used to predict the fatigue life of as-welded (AW) and HFMI-treated LS. A parametric study of the model was conducted for different steel grades to examine the impact of steel strength and HFMI parameters on fatigue life. The hardness method [15] was applied to describe local cyclic material behaviour for the AW and HFMI-treated conditions.

All these studies have in common that the notch strain approach is used to estimate the fatigue life under CAL. Verification of the strain approach for predicting the fatigue life of HFMI-treated components under VAL is still pending. This study focuses on the applicability of the strain approach to predict the fatigue life of HFMI-treated TS of S355 under VAL with a p(1/3) and a linear shaped spectrum. Experimental data were obtained from [8, 16, 17]. The approach estimating cyclic material behaviour via hardness is validated by comparing material parameters from the literature for both base material and HFMI-treated conditions. Considering the local HFMI-treatment conditions, weld toe geometry, compressive residual stresses and increased hardness, the fatigue life up to crack initiation is estimated, and appropriate conclusions were drawn.
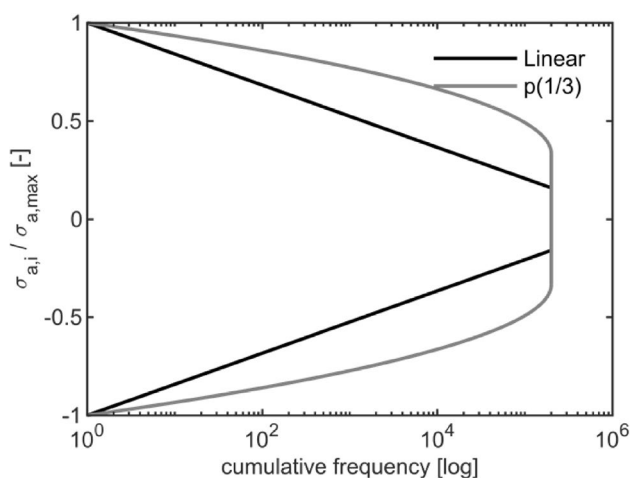
## 2 Experimental data

### 2.1 Considered load sequences and specimens

The applicability of the notch strain approach to predict the fatigue life of HFMI-treated welds was studied on TS fabricated out of mild steel (S355J2+N) subjected to uniaxial CA and VAL at a stress ratio of R = -1. The necessary data were extracted from the studies [8, 16, 17]. Within this investigation, the results from fatigue tests conducted under CAL and VAL with random loading sequences of a p(1/3) and linear shaped spectrum are incorporated. The considered stress spectra, load sequences and dimensions of the specimen are provided in Figs. 1, 2, and 3. The length for both spectra was set to y $L_S$= 2*10$^5$ load cycles.

### 2.2 Hardness measurements

The hardness distribution (HV0.1) was mapped on microsections. Figure 4 depicts the hardness distribution of the HFMI-treated weld toe and of the base plate to characterise the treated weld. The individual microstructures of the base material, the heat affected zone and the weld metal
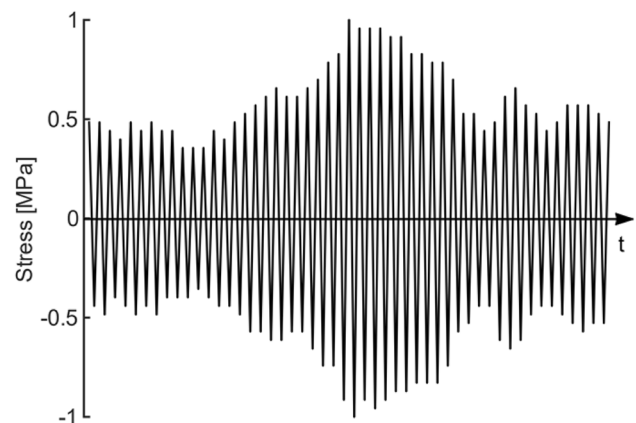
**Fig. 2** Random load sequence
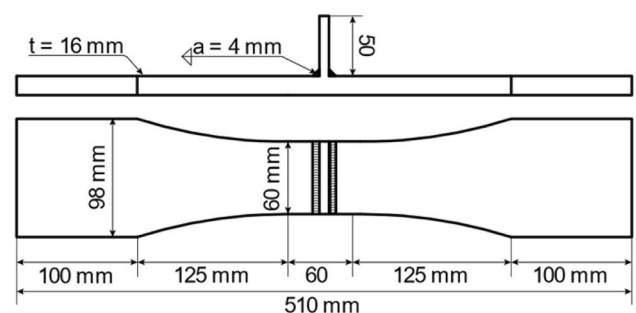
**Fig. 1** Stress spectra

**Fig. 3** Specimen type and dimension

are clearly distinguishable. At the base plate, a hardness of 170 HV was measured. The welding process and the HFMI treatment induce hardening at the weld toe, with hardness values reaching up to 346 HV. Similar values were measured for the base material S355J2+N as well as for the HFMI-treated weld area, as documented in [18].

As described in [16] and [17], the crack initiation and ultimate failure of the HFMI-treated TS originated from the base plate. The location of the crack initiation suggests that for HFMI-treated TS subjected to CAL and VAL at a stress ratio of R = -1, the fatigue strength of the base material determines the service life of the specimen. It is therefore assumed that the fatigue strength was locally increased by the HFMI treatment beyond the strength of the base material. To capture this effect numerically by applying the notch strain approach, the service life of the base material is estimated in addition to the service life of the HFMI-treated weld toe. The verification point for the base plate was defined 5 mm ahead of the weld toe. This point represents the mean value of the identified failure locations.

## 2.3 Weld toe geometry

Geometry measurements were conducted for all specimens using a 3D coordinate measuring system with a laser profile sensor (see Fig. 5a). The measurements were evaluated to identify the radius r of the weld toe, the flank angle θ, the throat thickness a and the side lengths $z_1$ and $z_2$ of the fillet, as displayed in Fig. 5b. For specimens in the HFMI-treated condition, the indentation depth t' was measured as well. The results of the geometry parameters measured are summarised in Table 1 for the specimens in the HFMI-treated condition. The mean value μ and standard deviation σ as well as the minimum and maximum measured values are given. The relative scatter is given by the variation coefficient v.

## 3 Notch strain approach

The notch strain concept can be found in various forms in the literature. These variants primarily differ in the methods applied to determine the local stresses and strains. For instance, extended notch root approximations are applied or different parameters are employed to assess the damage caused by individual stress–strain hysteresis. Within the various modifications, the notch strain approach is limited to describe the lifetime of components up to a defined crack length (typically 1 mm). Therefore, crack propagation cannot be described using this approach and is neglected in this study. The assessment is based on elastic–plastic stresses, which can be estimated from linear-elastic stresses using notch approximation methods (Neuber's rule). These linear elastic stresses are determined in finite element calculations.



**Fig. 4** Hardness distribution and depth of hardness profile of HFMI-treated weld toes
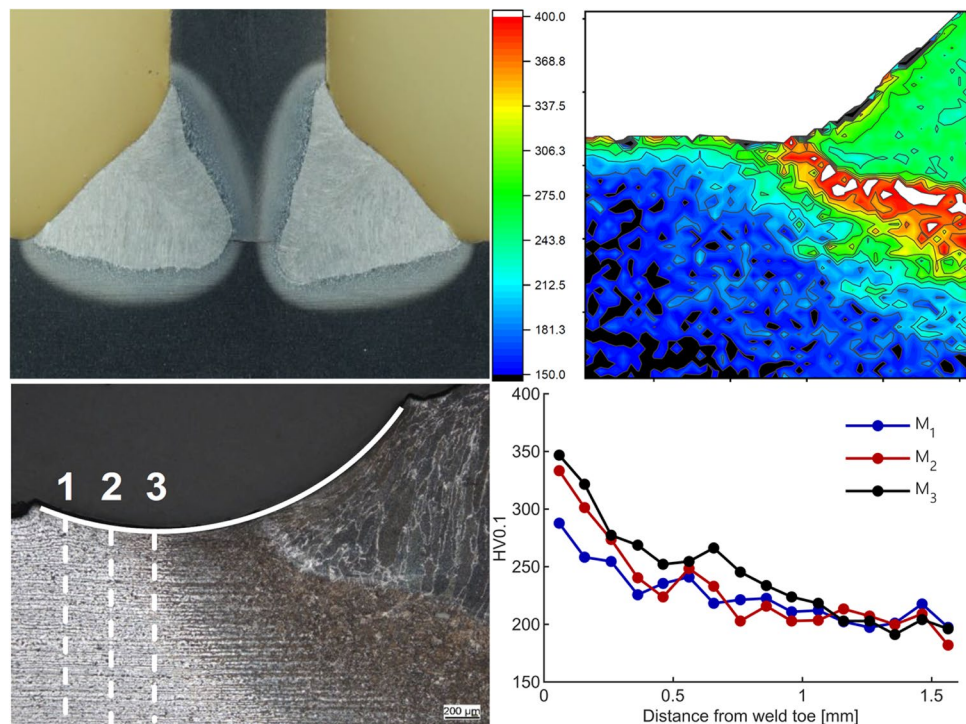
## 3.1 Determination of local linear-elastic stresses

As mentioned above, local linear–elastic stresses are calculated using a finite element method. The linear elastic notch stress history acting at the notch root is obtained by applying external nominal stresses. The welds were modelled using averaged geometry information of the weld. Based on the observed weld geometry, a 2D quadratic 8-node plane strain element model was generated considering a radius $r = r_{HFMI}$ and the measured indentation depth $t'_{HFMI}$ at the weld toe. In the HFMI-groove region, the number of elements was set to 15. The global element size was 1 mm. Due to significant angular distortion of 0.3° to 1.0° caused by welding, all specimens had to be straightened to be clamped into the test rig. The misalignment was minimised by using a three-point bending fixture, as shown in [17]. The imperfection between the clamping areas of the specimens was thus reduced. The angular distortion in other areas of the specimen was not affected by the straightening of the clamping areas. As shown by [19], angular imperfections may have a significant impact on local stresses. To address the interaction between the applied nominal load, the initial specimen distortion and the local stress field, the remaining angular misalignment was accounted for in the model, as shown in Fig. 6. When calculating the linear-elastic stresses, one side of the model was fixed. Subsequently, the clamping process was simulated via a given displacement u of the clamping jaws. Finally, a unit load of $\sigma_n = 1$ MPa was applied. This procedure was analogously adapted by [19]. Since all specimens studied, cracked at the base plate in front of the weld, linear elastic stresses were determined for the HFMI-zone and the base plate. The fatigue life is approximated separately for each



**Fig. 5** **a**) 3D coordinate measuring system and **b**) results of the measurements of transverse stiffeners made of S355 steel
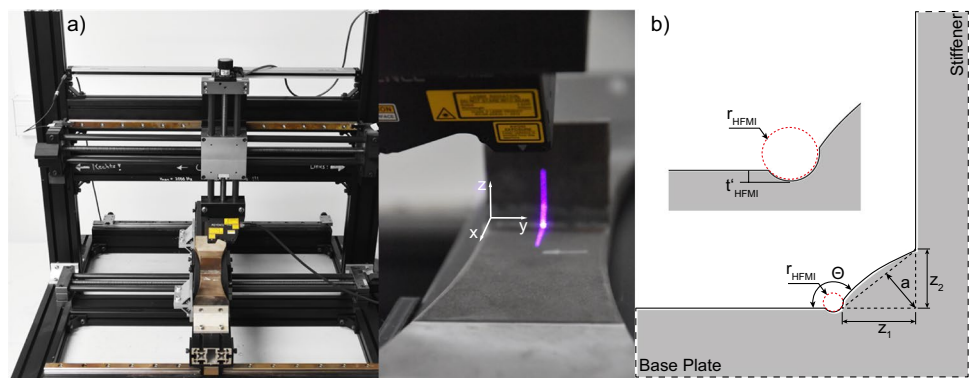
**Table 1** Mean values and standard deviations for geometric parameters derived from the measurements

| $r_{HFMI}$ [mm] | | | $t'_{HFMI}$ [mm] | | | $\Theta$ [°] | | | $|Z_1 - Z_2|$ [mm] | | | $a$ [mm] | | |
|---|---|---|---|---|---|---|---|---|---|---|---|---|---|---|
| μ | max | v | μ | max | v | μ | max | v | μ | max | v | μ | max | v |
| σ | min | [%] | σ | min | [%] | σ | min | [%] | σ | min | [%] | σ | min | [%] |
| 1.70 | 1.90 | 6.0 | 0.10 | 0.25 | 39.0 | 139.18 | 156.14 | 4.5 | 0.68 | 2.20 | 71.1 | 4.44 | 4.92 | 3.4 |
| 0.09 | 1.50 | | 0.04 | 0.04 | | 6.33 | 112.89 | | 0.48 | 0.00 | | 0.15 | 4.13 | |



**Fig. 6** Considered angular distortion, straightening of the specimen by clamping and subsequent loading
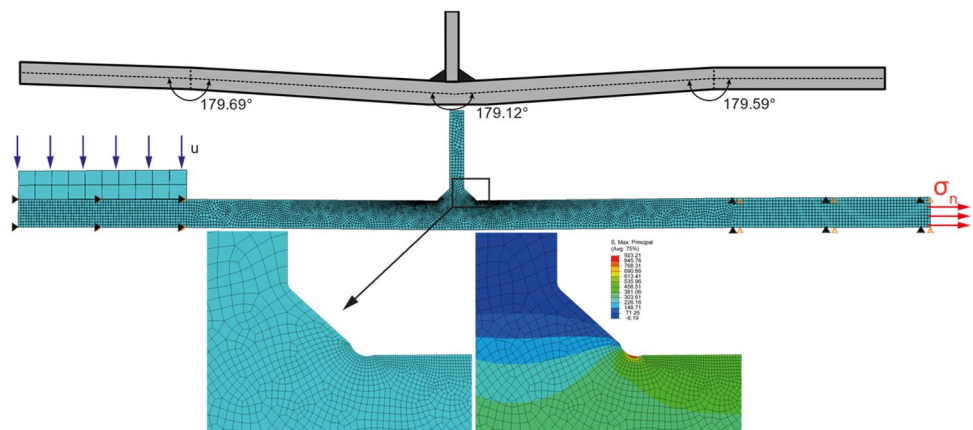
region. For the weld toe, a stress concentration factor (SCF) of $K_t = 2.45$ was obtained. At a distance 5 mm in front of the weld, the SCF is equal to $K_t = 1.3$.

## 3.2 Elastic–plastic material behaviour

For the determination of local elastic–plastic stresses and strains from the existing linear-elastic stresses, the uniaxial material deformation behaviour, described by the cyclic stress–strain curve according to the approach of Ramberg and Osgood [20], Eq. (2), must be known.

$$\varepsilon = \frac{\sigma}{E} + \left(\frac{\sigma}{K'}\right)^{\frac{1}{n'}}$$ (2)

The cyclic strain hardening coefficient K' and the cyclic strain hardening exponent n' are parameters used to describe the strain hardening behaviour of a material under cyclic loading conditions. These parameters can be determined experimentally through strain-controlled fatigue tests or incremental step tests on unnotched material specimens or estimated from quasistatic material properties. When dealing with locally inhomogeneous material dispersion, such as welded HFMI-treated components, it is important to consider the variations in material properties within different regions of the component.

Schubnell et al. [21] determined the cyclic properties of the heat affected zone (HAZ) and the base material of different steel grades, including S355J2+N. However, a direct determination of these material parameters is not possible for hardened surface layers, as sampling by common methods is not possible due to the low layer density (< 0.3 mm) and high hardness gradient [18]. In such cases, other approaches are often used to approximate the Ramberg-Osgood-material parameter K' und n'. By using the Lopez-Fatemi correlation [22], the cyclic stress–strain curve can be estimated via the hardness. This approach was applied in [18, 23] to estimate the fatigue life of HFMI-treated transverse stiffeners made of S355J2+N and is adopted in this study as well. In addition to the approach of estimating cyclic material properties by hardness, this study also uses data from the literature [23] for the material S355J2+N.

A comparison of approximated and experimentally estimated stress–strain curves for the base material (BM) and the HFMI-treated zone (HFMI) is shown in Fig. 7. According to [22], K' and n' can be approximated by Eq. (3) and Eq. (4) depending on the ratio between the ultimate strength $R_m$ and the yield strength $R_e$ for $R_m/R_e > 1.2$.

$$K' = 4.09 \cdot (HB) + 613$$ (3)

$$n' = -0.37 \cdot \log\left(\frac{0.75 \cdot R_e + 82}{1.16 \cdot R_m + 593}\right)$$ (4)
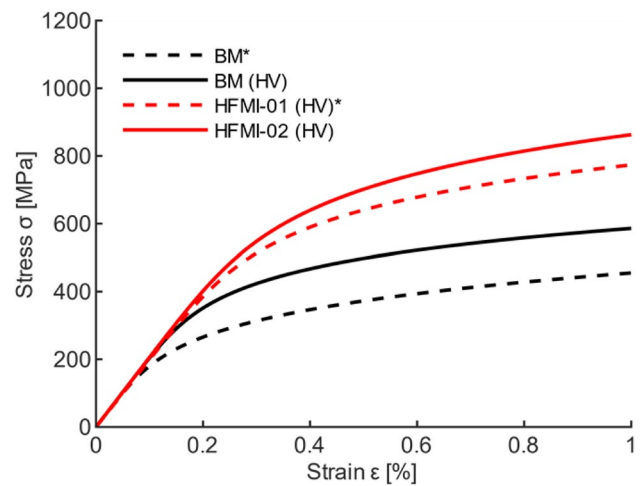


**Fig. 7** Cyclic stress–strain curves* estimated by [23] and approximated from hardness measurements [8]

with

$$R_e = 0.0039 \cdot HB^2 + 1.62 \cdot HB$$ (5)

$$R_m = \left(0.0012 \cdot HB^2 + 3.3 \cdot HB\right)$$ (6)

from [15]

The measured Vickers hardness can either be converted using DIN EN ISO 18265 [24] or determined using the Eq. (7) given in [10].

$$HV = 1.03 \cdot HB - 1.07$$ (7)

A hardness value of 170 HV was used for the BM and a hardness value of 346 HV for the HFMI-treated zone, based on the measurements described in section 2.2.

Once the cyclic stress–strain behaviour of the materials is characterised, the elastic stresses can be converted into local elastic–plastic stresses and strains using notch approximation methods. In the scope of the investigations of this study, the notch approximation method according to Neuber [25] was applied. Considering Masing behaviour [26] and material memory effects [27], the stress–strain paths can be numerically described for the considered loading sequence. In case a turning point of the load sequence is part of the initial load curve, the local elastic–plastic stresses can be determined according to Ramberg and Osgood, Eq. (2). For a load reversal, the elastic–plastic stresses are described by a hysteresis load according to the double Ramberg–Osgood curve, Eq. (8).

$$\Delta\varepsilon = \frac{\Delta\sigma}{E} + 2\left(\frac{\Delta\sigma}{2K'}\right)^{\frac{1}{n'}}$$ (8)

By setting Eqs. (2) and (8) in the notch approximation relation according to Neuber, the local elastic–plastic stresses σ and the stress range Δσ can be calculated according to Eqs. (9) and (10). For this purpose, the applied nominal stress $\sigma_n$ is multiplied by the elastic stress concentration factor $K_t$. Solving the equations requires an iterative approach.

$$\frac{\sigma}{E} + \left(\frac{\sigma}{K'}\right)^{\frac{1}{n'}} - \frac{(\sigma_n \cdot K_t)^2}{\sigma \cdot E} = 0 \tag{9}$$

$$\frac{\Delta\sigma}{E} + 2 \cdot \left(\frac{\Delta\sigma}{2K'}\right)^{\frac{1}{n'}} - \frac{(\Delta\sigma_n \cdot K_t)^2}{\Delta\sigma \cdot E} = 0 \tag{10}$$

When dealing with variable amplitude loading, the Masing and Memory model is essential for the complete description of the local stress–strain path. Therefore, closed hysteresis loops required for the calculation of damage parameters are identified using the HCM [27].

### 3.3 Fatigue damage parameter and linear damage accumulation

Within the present study, the parameter $P_{RAM}$ is used to calculate the damage for each closed hysteresis loop of the loading sequence. As stated in [10], $P_{RAM}$ is a modification of the $P_{SWT}$ according to Smith Watson Topper [28], considering a mean stress sensitivity of the material by the coefficient k. For the $P_{SWT}$ parameter, it is known that the influence of tensile mean stresses is underestimated, and the influence of compressive mean stresses is overestimated [29]. Thus, Bergmann [30] proposed extending the $P_{SWT}$ parameter with a material-dependent mean stress parameter k as follows:

$$P_{RAM} = \begin{cases} \sqrt{(\sigma_a + k \cdot \sigma_m) \cdot \varepsilon_a \cdot E} & for\ (\sigma_a + k \cdot \sigma_m) \geq 0 \\ 0 & for\ (\sigma_a + k \cdot \sigma_m) < 0 \end{cases} \tag{11}$$

The parameter k considers the mean stress sensitivity $M_\sigma$ depending on the material via Eq. (12) [31]. The ultimate strength $R_m$ of the material required for the calculation of $M_\sigma$ is determined via the hardness by Eq. (6).

$$k = \begin{cases} M_\sigma \cdot (M_\sigma + 2)\ for\ \sigma_m \geq 0 \\ \frac{M_\sigma}{3} \cdot \left(\frac{M_\sigma}{3} + 2\right) for\ \sigma_m < 0 \end{cases} \tag{12}$$

with

$$M_\sigma = 0.35 \cdot 10^{-3} \cdot R_m - 0.1 \tag{13}$$

The stress amplitude $\sigma_a$, the mean stress $\sigma_m$ and the strain amplitude $\varepsilon_a$ are determined for the observed hysteresis. The damage parameter Woehler curve required for damage

accumulation can be described by the correlation of the number of load cycles $N_i$ with the Coffin-Manson parameters $\sigma_f'$, $\varepsilon_f'$, b and c as well as the modulus of elasticity. To determine the Coffin-Manson parameters without mean stress effects, cyclic fatigue tests on material specimens are carried out at a stress or strain ratio of R = -1. Thus, Eq. (11) can be simplified to the $P_{SWT}$-Woehler curve, Eq. (14).

$$P_{RAM} = P_{SWT} = \sqrt{\sigma_f'^2 \cdot (2N)^{2b} + \sigma_f' \cdot \varepsilon_f' \cdot E \cdot (2N)^{b+c}} \tag{14}$$

Similar to the determination of the material parameters for the description of the elastic–plastic stress–strain behaviour, the parameters $\sigma_f'$, $\varepsilon_f'$, b and c must be specified for each material property at the weld toe. Alternatively, these values can be approximated via the hardness method [13] as applied in this study, Eqs. (15)-(18).

$$\sigma_f' = 4.25 \cdot HB + 225 \tag{15}$$

$$\varepsilon_f' = \left(0.32 \cdot HB^2 - 487 \cdot HB + 191000\right)/E \tag{16}$$

$$b = -0.09 \tag{17}$$

$$c = -0.56 \tag{18}$$

To reduce the computational effort of calculating the damage sums for long load sequences under VAL, the approach to describe a bilinear damage curve according to Wächter [32] was applied. The endurance limit was therefore set to $N_D = 5 \cdot 10^5$ according to UML [33] (Fig. 8).

### 3.4 Consideration of surface layer conditions

While the positive effect of the surface layer hardened by the HFMI treatment is considered in the stress–strain relation and the $P_{RAM}$-Woehler curves, the impact of the residual stresses has not yet been addressed. Residual stresses in the loading direction $\sigma_{RS}^T$ are not included in the original formulation of $P_{RAM}$. Schubnell et al. [34] addressed this by incorporating the residual stress into the mean stress during the damage calculation to quantify the influence of residual stresses on the crack initiation life (Eq. (19)).

$$P_{RAM} = \sqrt{\left(\sigma_a + k \cdot \left(\sigma_m + \sigma_{RS}^T\right) \cdot \varepsilon_a \cdot E\right)} \tag{19}$$

Recent studies [35–37] have shown that due to cyclic loading and single overload peaks, residual stresses may relax. It is therefore imperative to consider only those residual stresses remaining under cyclic loading. Equation (19) causes a shift of the stress–strain hysteresis downwards (residual compressive stress) and thus leads to a reduction of the damage. A similar evaluation of the residual stress state for HFMI-treated welds
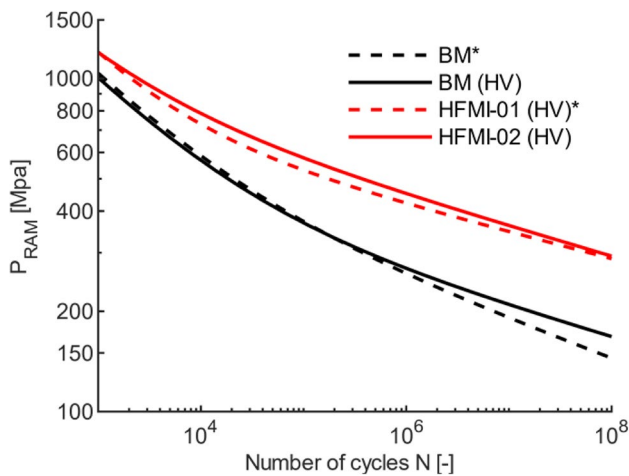
**Fig. 8** $P_{RAM}$-S-N curves for BM and HFMI.* estimated by [23] and approximated from hardness measurements [8]

roughness $R_z$ by Eq. (20). This approach is adopted to the FKM guideline "nonlinear" [31].

$$K_{R,P} = \left( 1 - 0,27 \cdot \log(R_z) \cdot \log\left( \frac{2 \cdot R_m}{400} \right) \right)^{0,43} \quad (20)$$

Within the damage calculation, this value of $K_{R,\,P}$ is incorporated by modifying the $P_{RAM}$-Woehler curves.

$$P_{RAM} = \frac{1}{K_{R,P}} \sqrt{\sigma_f'^2 \cdot (2N)^{2b} + \sigma_f' \cdot \varepsilon_f' \cdot E \cdot (2N)^{b+c}} \quad (21)$$

Additional influences from the component construction, such as statistical and fracture mechanics support factors $n_{bm}$ as described in [10, 31], are not addressed or considered in this study. It is assumed that the influence of $n_{bm}$ on the fatigue life estimation is marginal, as low stress gradients are expected at the weld toe and at the evaluation point on the base plate.

## 4 Results and discussion

For the applicability study of the notch strain approach, the results from studies were used. A summary of the selected data is shown in Table 2. In addition to the material and Coffin-Manson parameters estimated from the hardness, parameters from [23] were also used to evaluate the concept. Table 3 gives an overview of the input parameters applied to the base material and the HFMI-treated weld. The assessment presented is based on the simplification of applying each local material behaviour (BM, HFMI) to the entire model. As a more complex alternative the local cyclic material behaviour, approximated by the described method, can be assigned to each finite element based on the measured

has been previously conducted by [38] in the application of the 4R method. In the context of this work, the results of extensive studies [8, 37] on the stability of residual stresses are used.

As mentioned earlier, the examined specimens showed corroded surfaces adjacent to the weld seam, which is a result of the water jet cutting process. For all specimens of S355J2+N, failure was observed at the base plate, approximately 5 mm in front of the HFMI-treated weld toe [8, 16, 17]. This phenomenon indicates two possibilities. First, the fatigue strength of the weld was locally increased by the HFMI treatment beyond that of the base material. Second, the presence of the corroded surface may have led to additional stress concentrations and early crack initiation. In the FKM guideline [39], the influence of roughness can be taken into account via the mean surface

**Table 2** Overview of fatigue test data sets

| Data set | Reference | Specimen type | Material | R-ratio [-] | Spectrum | Loading sequence |
|---|---|---|---|---|---|---|
| No. 1 | [8] | Transverse stiffener | S355J2C+N | -1 | CAL | - |
| No. 2 | [16] | Transverse stiffener | S355J2C+N | -1 | VAL-p1/3) | random |
| No. 3 | [17] | Transverse stiffener | S355J2C+N | -1 | VAL-linear | random |

**Table 3** Material and input parameters

| Material condition | Hardness [HV] | Reference | E | $K'$ | $n'$ | $\sigma_f'$ | $\varepsilon_f'$ | b | c | $K_t$ | $R_z$ [µm] | $K_{R,P}$ |
|---|---|---|---|---|---|---|---|---|---|---|---|---|
| BM* | - | [23] | 204,933 | 1,351 | 0.224 | 1,291 | 0.442 | -0.115 | -0.54 | 1.3[1] | 75[2] | 0.79 |
| BM (HV) | 170 | - | 206,000 | 1,687 | 0.160 | 931 | 0.577 | -0.09 | -0.56 | 1.3[1] | 75[2] | 0.79 |
| HFMI (HV)* | - | [23] | 198,968 | 1,292 | 0.153 | 1,327 | 0.895 | -0.08 | -0.65 | 2.45[1] | - | 1.0 |
| HFMI (HV) | 346 | - | 206,000 | 1,991 | 0.160 | 1,657 | 0.307 | -0.09 | -0.56 | 2.45[1] | - | 1.0 |

1) Values from finite element analysis

2) Measured by contact stylus instruments

hardness indentations of the hardness map. This is followed by an elastic-plastic FE simulation. The considerable additional simulation and numerical calculation required by this alternative to determine the fatigue life by an elastic-plastic FE simulation does not necessarily lead to better agreement with the experimental test results, as shown in [10].

The fatigue life estimated with the adapted calculation algorithm presented in this study is shown in Fig. 9 to Fig. 11. These figures compare the calculated crack-initiation lifetime $N_{I,cal}$ and the experimental lifetime for the failure criteria fracture Nf,exp. The results using the Vickers

hardness of the HFMI-treated zone and base material can be taken from Figs. 9a–11a. In comparison, the calculated fatigue life applying the parameters given in [23] can be seen in Figs. 9b–11b. For data set 1 (Fig. 9), which was subjected to CAL, a good accuracy in the fatigue life prediction is achieved for the base material, with a slight overestimation in the range of $10^4$ to $10^5$ cycles.

It should be noted that the failure criteria are different. The calculated total service life including a crack propagation calculation can lead to larger values. Due to the low notch intensity at the base material, however, it is assumed

**Fig. 9** Calculated fatigue life of data set 1 (CAL) with Vickers hardness **a**) and with parameters from [23] **b**)
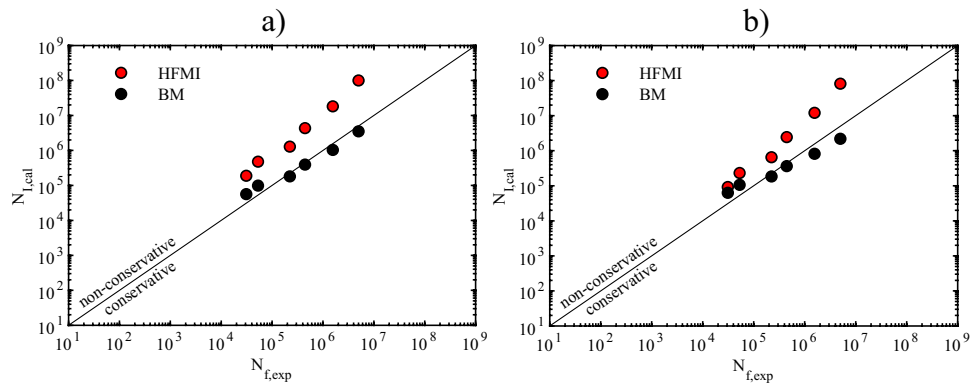
**Fig. 10** Calculated fatigue life of data set 2 (VAL p(1/3)) with Vickers hardness **a**) and with parameters from [23] **b**)
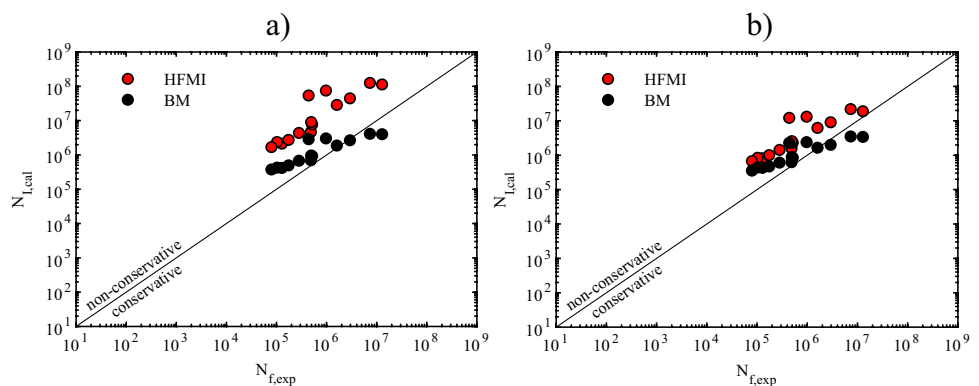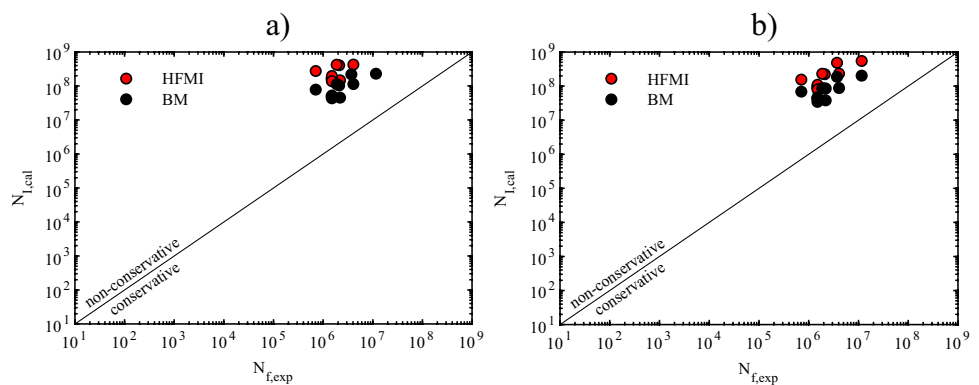
**Fig. 11** Calculated fatigue life of data set 3 (VAL linear) with Vickers hardness **a**) and with parameters from [23] **b**)

that the predominant part of the service life is determined by the crack initiation. For both sets of parameters applied, a similar lifetime is predicted for BM and HFMI subjected to CAL. The accuracy of the approach for the HFMI-treated zone cannot be evaluated, as all samples considered failed at the base plate. However, the results support the claim that the HFMI treatment increased the fatigue strength of the weld toe beyond that of the BM. This is reflected in the numerically determined higher number of cycles $N_{I,cal}$ for the HFMI-treated zone compared to the BM. The same effect can be observed in the results under VAL, Figs. 10–11.

For the random load sequence of the p(1/3)-spectrum, the lifetime for the BM in the regime $N \leq 10^6$ is overestimated, Fig. 10. This misestimation of the crack initiation life becomes evident when evaluating the results obtained from tests conducted with a linear-shaped spectrum. Figure 11 illustrates that the lifetime is generally significantly overestimated. Applying the parameters given in [23], lower numbers of cycles $N_{I,cal}$ are determined. However, even in this case, the assessment for both the HFMI-treated weld toe and the BM is unconservative. A possible explanation for the misestimation of service life is the omission of damage caused by smaller stresses in the cumulative damage accumulation. If the calculated damage parameter $P_{RAM}$ is smaller than the endurance strength at $N_D = 5 \cdot 10^5$ [33], the damage of the corresponding stress ranges is neglected. When comparing the linear spectrum to the p(1/3) spectrum in Fig. 1, smaller stress ranges occur much more frequently within the linear spectrum. Consequently, a greater deviation occurs between the experimentally determined and calculated service life for the linear spectrum in comparison to the p(1/3) spectrum. The overestimation of the fatigue life may also be related to the selection of the damage parameter. $P_{RAM}$, as a modification of $P_{SWT}$, evaluates the influence of sequence effects on the damage of each closed hysteresis based solely on the mean or residual stresses occurring at the notch. According to the literature [29] $P_{RAM}$ tends to overestimate the fatigue life for VAL when compressive residual stresses are present. Assuming base material behaviour, negligibly low residual stresses are observed. It can be assumed that the damage caused by a small cycle following a large cycle is not sufficiently taken into account. The sequence effect is partially covered by the notch root approximation and is consequently integrated into $P_{RAM}$. However, more pronounced sequence effects are inadequately captured using the damage parameter $P_{RAM}$ [29].

## 5 Conclusion and outlook

The applicability of a modified strain approach to predict the fatigue life of HFMI-treated transverse stiffeners under variable amplitude loading was studied. Modifications

to the approach included estimating the cyclic material parameters for the base material and the HFMI-treated zone via hardness [15, 22]. Elastic–plastic material behaviour was determined using the notch approximation according to Neuber. The required SCFs were determined by linear elastic finite element analysis considering the local and global geometry of the specimens. The parameter $P_{RAM}$ was used to calculate the damage for each closed hysteresis loop of the loading sequence considering residual stresses remaining during cyclic loading as well as the impact of surface roughness. The main conclusions of the work are as follows:

- In the case of CAL, a good accuracy in the fatigue life prediction is achieved for the BM, with a slight overestimation in the range of low cycle values and higher stresses. The accuracy of the approach for the HFMI-treated zone cannot be evaluated because for all test data considered, failure occurred at the base plate.
- Based on the results of the approach in conjunction with the experimental investigations, the conclusion that HFMI treatment increases the fatigue strength of the weld beyond that of the BM can be supported.
- For VAL, the approach yields unconservative results regarding lifetime prediction. As discussed in section 4, one reason for the inadequacy of lifetime prediction could be the choice of damage parameter.

Further investigations on the impact of the damage parameter for the assessment of HFMI-treated welded joints subjected to VAL are intended. It is therefore necessary to investigate how the endurance limit should be adjusted to adequately account for the damage caused by small stress ranges. To further validate the presented approach, additional experimental data must be incorporated. This requires verifying the reliability of the approach due to the influence of varying parameters such as material, notch geometry, stress ratio and spectrum shape.

## Declarations

**Conflict of interest** The authors declare no competing interests.

# References

1. Marquis GB, Barsoum Z (2016) IIW Recommendations for the HFMI treatment: for improving the fatigue strength of welded joints. IIW Collection. Springer Singapore, Singapore s.l

2. Kuhlmann U, Dürr A, Bergmann et al. (2006) Effizienter Stahlbau aus höherfesten Stählen unter Ermüdungsbeanspruchung: Fatigue strength improvement for welded high strength steel connections due to the application of post-weld treatment methods. Forschung für die Praxis / Forschungsvereiniung Stahlanwendung e.V. im Stahl-Zentrum, vol 620. Verl.- und Vertriebsges, Düsseldorf

3. Ummenhofer T, Herion S, Rack S et al (2011) REFRESH - Lebensdauerverlängerung bestehender und neuer geschweißter Stahlkonstruktionen: REFRESH - extension of the fatigue life of existing and new welded steel structures. In: Forschungsvohaben P 702. Forschungsvereinigung Stahlanwendung: Forschung für die Praxis, vol 702. Verl. und Vertriebsges. mbH, Düsseldorf

4. Yildirim HC, Marquis GB (2013) A round robin study of high-frequency mechanical impact (HFMI)-treated welded joints subjected to variable amplitude loading. Weld World. https://doi.org/10.1007/s40194-013-0045-3

5. Hobbacher A (2018) Recommendations for Fatigue Design of Welded Joints and Components, Softcover reprint of the original 2nd edition 2016. IIW Collection. Springer International Publishing; Springer, Cham

6. Leitner M, Gerstbrein S, Ottersböck MJ et al (2015) Fatigue Strength of HFMI-treated High-strength Steel Joints under Constant and Variable Amplitude Block Loading. Procedia Eng 101:251–258. https://doi.org/10.1016/j.proeng.2015.02.036

7. Leitner M, Stoschka M, Barsoum Z et al (2020) Validation of the fatigue strength assessment of HFMI-treated steel joints under variable amplitude loading. Weld World 64:1681–1689

8. Löschner D, Diekhoff P, Schiller R et al. (2020) Beanspruchungsreihenfolgeeinfluss auf die bearbeitungsbedingten Verfestigungen und Eigenspannungen und die Betriebsfestigkeit nachbehandelter Kerbdetails: Abschlussbericht zum Vorhaben IGF-Nr. 18.848 N. DVS Forschungsvereinigung, vol 455. DVS Media GmbH, Düsseldorf

9. Rudorffer W, Wächter M, Esderts A et al (2022) Fatigue assessment of weld seams considering elastic–plastic material behavior using the local strain approach. Welding in the World 66:721–730. https://doi.org/10.1007/s40194-021-01242-9

10. Rudorffer W, Wächter M, Esderts A et al. (eds) (2022) Nichtlinearer Nachweis für Schweißnähte – Ein Vorschlag zur Erweiterung der FKM-Richtlinie Nichtlinear. Deutscher Verband für Materialforschung und –prüfung e.V

11. Lihavainen V-M, Marquis G (2006) Fatigue Life Estimation of Ultrasonic Impact Treated Welds Using a Local Strain Approach. Steel Res Int 77:896–900. https://doi.org/10.1002/srin.200606478

12. Dürr A (2007) Zur Ermüdungsfestigkeit von Schweißkonstruktionen aus höherfesten Baustählen bei Anwendung von UIT-Nachbehandlung. Zugl.: Stuttgart, Univ., Diss., 2006. Mitteilungen/Institut für Konstruktion und Entwurf, vol 2006,3. Univ; Inst. für Konstruktion und Entwurf, Stuttgart, Stuttgart

13. Seeger T, Heuler P (1984) Ermittlung und Bewertung örtlicher Beanspruchungen zur Lebensdauerabschätzung schwingbelasteter Bauteile. Bericht FF-20

14. Fuštar B, Lukačević I, Skejić D et al (2021) Two-Stage Model for Fatigue Life Assessment of High Frequency Mechanical Impact (HFMI) Treated Welded Steel Details. Metals 11:1318. https://doi.org/10.3390/met11081318

15. Roessle M (2000) Strain-controlled fatigue properties of steels and some simple approximations. Int J Fatigue 22:495–511. https://doi.org/10.1016/S0142-1123(00)00026-8

16. Schiller R, Löschner D, Diekhoff P et al (2021) Sequence effect of p(1/3) spectrum loading on service fatigue strength of as-welded and high-frequency mechanical impact (HFMI)-treated transverse stiffeners of mild steel. Welding in the World 65:1821–1839. https://doi.org/10.1007/s40194-021-01121-3

17. Löschner D, Schiller R, Diekhoff P et al (2022) Sequence effect of as-welded and HFMI-treated transverse attachments under variable loading with linear spectrum. Weld World. https://doi.org/10.1007/s40194-022-01302-8

18. Luke M, Ummenhofer T, Farajan M et al. (2020) Rechnergestütztes Bewertungskonzept zum Nachweis der Lebensdauerverlängerung von mit dem Hochfrequenz-Hämmerverfahren (HFMI) behandelten Schweißverbindungen aus hochfesten Stählen. Berichtszeitraum 1.1.2017 - 31.12.2019. Abschlussbericht 20.05.2020

19. Ottersböck M, Leitner M, Stoschka M (2018) Impact of Angular Distortion on the Fatigue Performance of High-Strength Steel T-Joints in as-Welded and High Frequency Mechanical Impact-Treated Condition. Metals 8:302. https://doi.org/10.3390/met8050302

20. Ramberg W, Osgood WR (1943) Description of stress-strain curves by three parameters. Technical note/National Advisory Committee for Aeronautics, vol 902. National Advisory Committee for Aeronautics, Washington D.C.

21. Schubnell J, Discher D, Farajian M (2019) Determination of the static, dynamic and cyclic properties of the heat affected zone for different steel grades. Mater Test 61:635–642. https://doi.org/10.3139/120.111367

22. Lopez Z, Fatemi A (2012) A method of predicting cyclic stress–strain curve from tensile properties for steels. Mater Sci Eng A 556:540–550. https://doi.org/10.1016/j.msea.2012.07.024

23. Schubnell J (2021) Experimentelle und numerische Untersuchung des Ermüdungsverhaltens von verfestigten Kerben und Schweißverbindungen nach dem Hochfrequenzhämmern. Karlsruher Institut für Technologie (KIT). https://doi.org/10.5445/IR/1000135869

24. DIN EN ISO 18265:2014-02, Metallische Werkstoffe_- Umwertung von Härtewerten (ISO_18265:2013); Deutsche Fassung EN_ISO_18265:2013

25. Neuber H (1961) Theory of Stress Concentration for Shear-Strained Prismatical Bodies With Arbitrary Nonlinear Stress-Strain Law. J Appl Mech 28:544–550. https://doi.org/10.1115/1.3641780

26. Masing G Eigenspannungen und Verfestigung beim Messing. In: Proc. 2nd Int. Cong. of Appl. Mech. pp 332–335, Zürich

27. Clormann UH, Seeger T (1986) Rainflow-HCM. Ein Zählverfahren für Betriebsfestigkeitsnachweise auf werkstoffmechanischer Grundlage. Stahlbau, Der 55

28. Smith KN, Watson P, Topper TH (1969) A stress-strain function for the fatigue of metals. Report / Solid Mechanics Division, University of Waterloo, vol 21, Waterloo, Ontario

29. Haibach E (2006) Betriebsfestigkeit: Verfahren und Daten zur Bauteilberechnung, 3., korrigierte und ergänzte Auflage. VDI-Buch. Springer, Berlin

30. Bergmann JW (1983) Zur Betriebsfestigkeitsbemessung gekerbter Bauteile auf der Grundlage der örtlichen Beanspruchungen. Darmstadt, Techn. Hochsch., Fachbereich Konstruktiver Ingenieurbau, Diss. A

31. Fiedler M, Wächter M, Varfolomeev I et al (2019) Richtlinie Nichtlinear: Rechnerischer Festigkeitsnachweis unter expliziter Erfassung nichtlinearen Werkstoffverformungsverhaltens ; für Bauteile aus Stahl, Stahlguss und Aluminiumknetlegierungen, 1. Auflage. FKM-Richtlinie. VDMA Verlag GmbH, Frankfurt am Main

32. Wächter M (2016) Zur Ermittlung von zyklischen Werkstoffkennwerten und Schädigungsparameterwöhlerlinien. Universitätsbibliothek der TU Clausthal

33. Boller C, Seeger T (1990) Materials data for cyclic loading. In: Materials science monographs, vol 61. Elsevier, Amsterdam

34. Schubnell J, Pontner P, Wimpory RC et al (2020) The influence of work hardening and residual stresses on the fatigue behavior of high frequency mechanical impact treated surface layers. Int J Fatigue 134:105450. https://doi.org/10.1016/j.ijfatigue.2019.105450

35. Leitner M, Khurshid M, Barsoum Z (2017) Stability of high frequency mechanical impact (HFMI) post-treatment induced residual stress states under cyclic loading of welded steel joints. Eng Struct 143:589–602. https://doi.org/10.1016/j.engstruct.2017.04.046

36. Schubnell J, Carl E, Farajian M et al (2020) Residual stress relaxation in HFMI-treated fillet welds after single overload peaks.

Welding in the World 64:1107–1117. https://doi.org/10.1007/s40194-020-00902-6

37. Löschner D, Diekhoff P, Schiller R et al (2023) Residual stress stability of HFMI-treated transverse attachments under variable amplitude loading with the P(1/3) and the linear spectrum. Welding in the World 67:1545–1557. https://doi.org/10.1007/s40194-023-01491-w

38. Ahola A, Muikku A, Braun M et al (2021) Fatigue strength assessment of ground fillet-welded joints using 4R method. Int J Fatigue 142:105916. https://doi.org/10.1016/j.ijfatigue.2020.105916

39. Forschungskuratorium Maschinenbau, VDMA Verlag GmbH (2021) Analytical strength assessment of components: Made of steel, cast iron and aluminium materials : FKM guideline, 7th revised edition 2020. VDMA Verlag GmbH, Frankfurt am Main, FKM Forschung im VDMA